

Rayleigh-Brillouin scattering in binary mixtures of disparate-mass constituents: SF₆-He, SF₆-D₂, and SF₆-H₂

Yuanqing Wang and Wim Ubachs *Department of Physics and Astronomy, LaserLab, Vrije Universiteit, De Boelelaan 1081, 1081 HV Amsterdam, The Netherlands*Cesar A. M. de Moraes  and Wilson Marques Jr. *Departamento de Física, Universidade Federal do Paraná, Caixa Postal 19044, Curitiba 81531-990, Brazil*

(Received 3 July 2020; accepted 16 December 2020; published 5 January 2021)

The spectral distribution of light scattered by microscopic thermal fluctuations in binary mixture gases was investigated experimentally and theoretically. Measurements of Rayleigh-Brillouin spectral profiles were performed at a wavelength of 532 nm and at room temperature, for mixtures of SF₆-He, SF₆-D₂, and SF₆-H₂. In these measurements, the pressure of the gases with heavy molecular mass (SF₆) is set at 1 bar, while the pressure of the lighter collision partner was varied. In view of the large polarizability of SF₆ and the very small polarizabilities of He, H₂, and D₂, under the chosen pressure conditions these low mass species act as spectators and do not contribute to the light scattering spectrum, while they influence the motion and relaxation of the heavy SF₆ molecules. A generalized hydrodynamic model was developed that should be applicable for the particular case of molecules with heavy and light disparate masses, as is the case for the heavy SF₆ molecule, and the lighter collision partners. Based on the kinetic theory of gases, our model replaces the classical Navier-Stokes-Fourier relations with constitutive equations having an exponential memory kernel. The energy exchange between translational and internal modes of motion is included and quantified with a single parameter z that characterizes the ratio between the mean elastic and inelastic molecular collision frequencies. The model is compared with the experimental Rayleigh-Brillouin scattering data, where the value of the parameter z is determined in a least-squares procedure. Where very good agreement is found between experiment and the generalized hydrodynamic model, the computations in the framework of classical hydrodynamics strongly deviate. Only in the hydrodynamic regime both models are shown to converge.

DOI: [10.1103/PhysRevE.103.013102](https://doi.org/10.1103/PhysRevE.103.013102)

I. INTRODUCTION

Spontaneous Rayleigh-Brillouin (RB) scattering spectra of gaseous and fluidic media contain information on the thermodynamics and the transport properties of the gases and fluids such as thermal diffusivity, speed of sound, relaxation times of various dynamical processes, etc. [1–3]. In addition, such spectra provide a way to test a given theory of the energy relaxation dynamics in gases, and in gaseous mixtures. Theories of RB scattering for fluids in the kinetic and hydrodynamic regimes have been devised based on the linearized Boltzmann equation and on linearized hydrodynamic equations, respectively. Many models have already successfully explained the scattered light spectra [4–6]. Some models have accomplished reproducing the spectra very well, even though some discrepancies with experiments still exist, while their validity is often restricted to certain pressure regimes.

A celebrated example of a model representation of RB-scattering profiles in the kinetic regime is the Tenti model [7,8], which was applied to describe the spectral profiles of a variety of gases, such as N₂ [9], CO₂ [10,11], and N₂O [12]. However, the Tenti model was not developed for modeling the RB spectra of mixture gases. Moreover, it requires as input the values of the macroscopic transport coefficients, such as

heat capacity, thermal conductivity, specific heat ratio, and shear viscosity, in general not known for composite mixtures. And ultimately the value of the bulk viscosity, the parameter determining internal relaxation, is typically determined via a fitting procedure when applying the Tenti model. This makes the Tenti model not immediately applicable to the present case of binary mixtures.

The hydrodynamic theory of light scattering in binary fluid mixtures was first developed by Mountain and Deutch [13], who described the local dielectric constant fluctuations by several linear hydrodynamic equations including the continuity equation for mass conservation, the Navier-Stokes equation for momentum conservation, the diffusion equation, and the energy transport equation. Later, Cohen *et al.* [14] corrected some correlation functions by adding the “non-Lorentzian” term based on the original paper of Mountain and Deutch [13] therewith improving the light scattering models.

On the experimental side Rayleigh-Brillouin scattering spectra of helium-xenon atomic gas mixtures were measured by Letamendia *et al.* [15] at different pressures, compositions, and scattering angles. The data were compared with a complete two-component hydrodynamic theory and good agreement was found at low molar fractions of He and at molar fractions of He higher than a “critical” value which

depends on the partial pressure of Xe. In addition, since the spectral shape in He-Xe mixtures is very sensitive to the presence and magnitude of thermal-diffusion effects, the thermal diffusion coefficient could be derived. A kinetic model was formulated by Letamendia *et al.* [16] based on the generalized Enskog equations for a binary mixture of hard-sphere fluids. This model gives an improvement over an existing model derived by Boley and Yip [17], which is based on the linearized Boltzmann equations for Maxwell molecules and which was successful in explaining light scattering spectra of He-Xe mixtures at very low Xe pressure and small Xe molar fraction, conditions under which imperfect-gas effects and thermal diffusion can be ignored.

Bonato and Marques Jr. [18] proposed a model to describe the spontaneous density fluctuations in a binary mixture of monatomic ideal gases based on the Boltzmann equation, the collision operators of which are replaced by simple relaxation-time terms. For this model, the description of kinetic equations for a mixture of monatomic ideal gases is characterized by the fields of partial number density, partial flow velocity and partial temperature, and assuming that the particles of the mixture interact according to the Lennard-Jones (6–12) potential. This model was applied to the light scattering spectrum of a binary gas mixture passing over from a hydrodynamic to a kinetic regime. The measurements by Gu *et al.* [19] of RB spectra on mixtures of Ar-He and Kr-He, were found to produce excellent agreement with this model. Clearly, since noble gas atoms do not have the internal degrees of motion that molecules have, this model is not suited for mixtures including molecular gases.

In order to extend these studies into the molecular regime by including intramolecular as well as intermolecular relaxation, RB scattering of mixtures of SF₆-He, SF₆-D₂, SF₆-H₂ is measured under different conditions. A relaxation hydrodynamic model for these mixtures of specific disparate masses is developed, based on a generalized hydrodynamic description, and a comparison will be made between the experimental data and the model developed. Also a comparison will be made with a classical hydrodynamics model.

II. RELAXATION HYDRODYNAMIC MODEL FOR BINARY MIXTURES

In a fluid in thermal equilibrium, the intensity of the Rayleigh-Brillouin scattered light is related to the fluctuations of the dielectric constant $\delta\epsilon$ caused by the random thermal motion of molecules [20]. For a binary gas mixture these fluctuations are related to the fluctuations of thermodynamic variables as pressure p , temperature T , and mass concentration of one constituent c :

$$\delta\epsilon(\mathbf{r}, t) = \left(\frac{\partial\epsilon}{\partial p} \right)_{T,c} \delta p(\mathbf{r}, t) + \left(\frac{\partial\epsilon}{\partial T} \right)_{p,c} \delta T(\mathbf{r}, t) + \left(\frac{\partial\epsilon}{\partial c} \right)_{p,T} \delta c(\mathbf{r}, t), \quad (1)$$

and the dynamic structure factor provides an expression from which the scattering spectrum can be computed:

$$S(\mathbf{q}, \omega) = 2\text{Re}[\langle \delta\epsilon(\mathbf{q}, i\omega) \delta\epsilon(-\mathbf{q}, 0) \rangle], \quad (2)$$

where \mathbf{q} represents the scattering vector with magnitude:

$$q = 2k_i \sin \frac{\theta}{2} = \frac{4\pi n}{\lambda_i} \sin \frac{\theta}{2}, \quad (3)$$

with k_i and λ_i the wave vector and wavelength of the incident light, n the refractive index, and θ the scattering angle [21]. This sets the dependence of the dynamic structure factor on the experimental conditions.

In classical mixture theory [13,14], the macroscopic state of a binary gas mixture is characterized by the six scalar fields of mass density $\rho = \rho_1 + \rho_2$, flow velocity \mathbf{v} (contributing a field for each direction), temperature T , and mass concentration $c = \rho_1/\rho$, where the index 1 refers to light constituent, while the index 2 refers to the heavy one. The balance equations governing the dynamical behavior of these fields are as follows.

(1) The continuity equation:

$$\frac{d\rho}{dt} + \rho \nabla \cdot \mathbf{v} = 0, \quad (4)$$

(2) the momentum equation:

$$\rho \frac{d\mathbf{v}}{dt} + \nabla \cdot \boldsymbol{\sigma} = 0, \quad (5)$$

(3) the diffusion equation:

$$\rho \frac{dc}{dt} + \nabla \cdot \mathcal{J} = 0, \quad (6)$$

(4) the energy transport equation:

$$\rho \frac{d\varepsilon}{dt} + \nabla \cdot \boldsymbol{\kappa} + \boldsymbol{\sigma} : \nabla \mathbf{v} = 0, \quad (7)$$

where $\boldsymbol{\sigma}$ is the pressure tensor, ε is the mixture specific internal energy, $\boldsymbol{\kappa}$ is the heat flux vector, and \mathcal{J} is the diffusion flux of the light constituent in the mixture, while $d/dt = \partial/\partial t + \mathbf{v} \cdot \nabla$ denotes the material time derivative. The balance equations (4)–(7) become a closed set of field equations for the determination of the basic fields if we provide constitutive relations for the pressure tensor, the heat flux vector, and the diffusion flux. In the Navier-Stokes-Fourier approximation, these constitutive relations are [22]

(i) the Navier-Stokes law,

$$\boldsymbol{\sigma} = (p - \eta_b \nabla \cdot \mathbf{v}) \mathbf{I} - 2 \eta_s \overset{\circ}{\nabla} \mathbf{v}, \quad (8)$$

where p is the mixture pressure, η_b is the volume (or bulk) viscosity, η_s is the shear viscosity, and $\overset{\circ}{\nabla} \mathbf{v}$ is rate-of-shear tensor;

(ii) the Fourier law of heat conduction,

$$\boldsymbol{\kappa} = -\lambda_{\text{th}} \nabla T + \left[\mu - T \left(\frac{\partial\mu}{\partial T} \right)_{p,c} + k_T \left(\frac{\partial\mu}{\partial c} \right)_{p,T} \right] \mathcal{J}, \quad (9)$$

where λ_{th} is the thermal conductivity of the mixture, k_T is the thermal diffusion ratio [23], and $\mu = \mu_1/m_1 - \mu_2/m_2$ is the mixture chemical potential (i.e., the difference in the chemical potential per unit mass of the two constituents);

(iii) the Fick law of diffusion,

$$\mathcal{J} = -\rho D_{12} \left[\nabla c + \frac{k_p}{p} \nabla p + \frac{k_T}{T} \nabla T \right], \quad (10)$$

where D_{12} is the diffusion coefficient and $k_p = -(p/\rho^2)(\partial\rho/\partial c)_{p,T}/(\partial\mu/\partial c)_{p,T}$ is the so-called barodiffusion factor.

As pointed out in the literature [24], the description of time-dependent processes based on the Navier-Stokes-Fourier theory starts to deviate from experimental data at high frequencies, such as in the case of Rayleigh-Brillouin scattering, where typically hypersound frequencies come into play. In order to overcome this situation, we may consider a generalization of the Navier-Stokes-Fourier constitutive relations by assuming that the pressure tensor, the heat flux vector, and the diffusion flux respond to gradients only after a relaxation time has elapsed. Such type of approach was first introduced by Cattaneo [25] to address the paradox of heat conduction in single fluid which follows from Fourier's law and it leads to a constitutive equation for the heat flux vector with an exponential memory kernel. In the present paper, our generalized constitutive equations follow from the kinetic theory proposed by Alievskii and Zhdanov [26] for a mixture of polyatomic gases. Basing on Grad's moment method [27], a macroscopic state of a mixture is characterized by the basic fields of partial mass densities, partial diffusion fluxes, partial stress tensors, partial specific energies, and partial heat fluxes associated with translational and internal molecular degrees of freedom.

A closed system of linear field equations for the determination of the basic fields can be obtained if we multiply the Boltzmann equation for a polyatomic gas mixture by an appropriate set of Hermite and internal energy polynomials, integrate over peculiar velocities, and sum over internal states. The collision integrals appearing in these equations can be expressed in terms of the basic fields by considering the so-called 17-moment approximation to the distribution function. In the case of a binary gas mixture, where the molecular mass ratio m_1/m_2 is a small parameter and the exchange of energy between translational and internal degrees of freedom of the molecules is a slow process, this system of field equations becomes fully decoupled and its solution can be used to derive the following constitutive relations:

$$\boldsymbol{\sigma} = \left(p - \int_0^t \eta_b(t-t') \nabla \cdot \mathbf{v}(\mathbf{r}, t') dt' \right) \mathbf{I} - 2[\eta_s]_1 \overset{\circ}{\nabla} \mathbf{v} - 2 \int_0^t [\eta_s]_2(t-t') \overset{\circ}{\nabla} \mathbf{v}(\mathbf{r}, t') dt', \quad (11)$$

$$\boldsymbol{\kappa} = -[\lambda_{th}]_1 \nabla T - \int_0^t [\lambda_{th}]_2(t-t') \nabla T(\mathbf{r}, t') dt' + \left[\mu - T \left(\frac{\partial \mu}{\partial T} \right)_{p,c} + k_T \left(\frac{\partial \mu}{\partial c} \right)_{p,T} \right] \mathcal{J}, \quad (12)$$

$$\mathcal{J} = -\rho \int_0^t D_{12}(t-t') \left[\nabla c(\mathbf{r}, t') + \frac{k_p}{p} \nabla p(\mathbf{r}, t') + \frac{k_T}{T} \nabla T(\mathbf{r}, t') \right] dt', \quad (13)$$

where the generalized transport coefficients are defined as

$$\eta_b(t-t') = \eta_b \frac{e^{-(t-t')/\tau_v}}{\tau_v}, \quad (14)$$

$$[\eta_s]_2(t-t') = [\eta_s]_2 \frac{e^{-(t-t')/\tau_2}}{\tau_2}, \quad (15)$$

$$[\lambda_{th}]_2(t-t') = [\lambda_{th}^{tr}]_2 \frac{e^{-(t-t')/\tau_2'} + [\lambda_{th}^{int}]_2 \frac{e^{-(t-t')/\tau_2''}}{\tau_2''}, \quad (16)$$

$$D_{12}(t-t') = D_{12} \frac{e^{-(t-t')/\tau_w}}{\tau_w}. \quad (17)$$

It is clear that our generalized constitutive relations depend on exponential memory kernels which are connected with the characteristic relaxation times τ_v , τ_2 , τ_2' , τ_2'' , and τ_w that give us, respectively, a measure of time interval spent by dynamic pressure, partial stress tensors, partial heat fluxes, and diffusion flux to achieve a stationary value.

Insertion of the constitutive relations (11)–(13) into the conservation equations (4)–(7) leads to a linear system of field equations. As (p, c, T) is not a set of statistically independent variables, here it is replaced by (ϕ, p, c) with

$$\phi = T - \frac{T_0 \beta_T}{\rho_0 c_p} p,$$

where $\beta_T = -\rho_0^{-1}(\partial\rho/\partial T)_{p,c} = T_0^{-1}$ and $c_p = (\partial\varepsilon/\partial T)_{\rho,c} + T_0(\partial p/\partial T)_{\rho,c}^2/\rho_0^2(\partial p/\partial\rho)_{T,c}$ are the thermal expansion coefficient and the specific heat capacity at constant pressure, respectively. Equilibrium values are denoted by the subscript zero, while thermodynamics derivatives are understood to be evaluated at equilibrium. After Fourier-Laplace transformations, this linear system for macroscopic fluctuations can be rewritten as

$$\mathbf{A}\boldsymbol{\psi}(\mathbf{q}, s) = \mathbf{B}\boldsymbol{\psi}(\mathbf{q}, 0), \quad (18)$$

where

$$\boldsymbol{\psi} = \begin{pmatrix} \psi_1 \\ \psi_2 \\ \psi_3 \\ \psi_4 \end{pmatrix} = \begin{pmatrix} \beta_T \bar{\phi} \\ \bar{c} \\ \bar{p}/p_0 \\ \tau_s \nabla \cdot \bar{\mathbf{v}} \end{pmatrix}, \quad (19)$$

and the 4×4 matrices \mathbf{A} and \mathbf{B} have the form,

$$\mathbf{A} = \begin{pmatrix} s + f(s)q^2 & -s \frac{\gamma-1}{\gamma} \rho_0 \frac{k_T}{p_0} \left(\frac{\partial \mu}{\partial c} \right)_{p,T} & \frac{\gamma-1}{\gamma} f(s)q^2 & 0 \\ k_T g(s)q^2 & s + g(s)q^2 & \mathcal{P} k_p g(s)q^2 & 0 \\ -s\gamma & -s\gamma \rho_0 \frac{k_p}{p_0} \left(\frac{\partial \mu}{\partial c} \right)_{p,T} & s & \gamma \\ 0 & 0 & -q^2 & s + b(s)q^2 \end{pmatrix}, \quad (20)$$

$$\mathbf{B} = \tau_s \begin{pmatrix} 1 & -\frac{(\gamma-1)}{\gamma} \rho_0 \frac{k_T}{p_0} \left(\frac{\partial \mu}{\partial c} \right)_{p,T} & 0 & 0 \\ 0 & 1 & 0 & 0 \\ -\gamma & -\gamma \rho_0 \frac{k_p}{p_0} \left(\frac{\partial \mu}{\partial c} \right)_{p,T} & 1 & 0 \\ 0 & 0 & 0 & 1 \end{pmatrix}. \quad (21)$$

TABLE I. The dynamic polarizabilities α (given in units of 10^{-40} C m²/V) at wavelength of 532.22 nm were calculated based on the static polarizability and the dynamic polarizability function [29], and the used values as cited in footnotes. Heat capacity ratio γ for the molecular species as obtained from experiment.

Molecule	α	γ
SF ₆	5.029 ^a	1.10 ^d
He	0.231 ^b	1.66 ^e
D ₂	0.900 ^c	1.40 ^e
H ₂	0.911 ^c	1.41 ^e

^aReference [30].

^bReference [31].

^cReference [32].

^dReference [33].

^eReference [34].

In the above expressions, time is given in units of the stress relaxation time:

$$\tau_s = ([\eta_s]_1 + [\eta_s]_2)/p = \eta_s/p, \quad (22)$$

and length is given in units of the mixture mean free path $\tau_s\sqrt{p_0/\rho_0}$. The specific heat capacity ratio of the mixture,

$$\gamma = 1 + [x_1/(\gamma_1 - 1) + x_2/(\gamma_2 - 1)]^{-1}, \quad (23)$$

can be calculated from the specific heat ratios γ_i (as listed in Table I) and the molar fractions x_i of the constituents. In the above matrices the following functional forms are represented:

$$\mathcal{P} = 1 + \frac{\gamma - 1}{\gamma} \frac{k_T}{k_p}, \quad (24)$$

$$\mathbf{g}(s) = \frac{\rho_0 D_{12}}{\eta_s} \frac{\tau_s/\tau_w}{s + \tau_s/\tau_w}, \quad (25)$$

$$f(s) = \frac{[\lambda_{th}]_1}{\eta_s c_p} + \frac{[\lambda_{th}^{tr}]_2}{\eta_s c_p} \frac{\tau_s/\tau'_2}{s + \tau_s/\tau'_2} + \frac{[\lambda_{th}^{int}]_2}{\eta_s c_p} \frac{\tau_s/\tau''_2}{s + \tau_s/\tau''_2}, \quad (26)$$

$$b(s) = \frac{4}{3} \frac{[\eta_s]_1}{\eta_s} + \frac{4}{3} \frac{[\eta_s]_2}{\eta_s} \frac{\tau_s/\tau_2}{s + \tau_s/\tau_2} + \frac{\eta_b}{\eta_s} \frac{\tau_s/\tau_v}{s + \tau_s/\tau_v}. \quad (27)$$

Note that the light scattering predictions of the classical mixture theory derived by Mountain and Deutch [13] follows from our generalized hydrodynamic model if we set the functions appearing in matrix \mathbf{A} as

$$\mathbf{g}(s) = \frac{\rho_0 D_{12}}{\eta_s}, \quad (28)$$

$$f(s) = \frac{[\lambda_{th}]_1 + [\lambda_{th}^{tr}]_2 + [\lambda_{th}^{int}]_2}{\eta_s c_p}, \quad (29)$$

$$b(s) = \frac{4}{3} + \frac{\eta_b}{\eta_s}. \quad (30)$$

For the computation of the RB-spectral profiles the matrix equation can be further evaluated. This can be done, both for the relaxation hydrodynamics model taking the functional forms for $\mathbf{g}(s)$, $f(s)$, and $b(s)$ as defined in Eqs. (25)–(27), as well as for the classical hydrodynamics model, by taking the forms defined in Eqs. (28)–(30). Here we proceed by evaluating the more complex case for the relaxation hydrodynamics

model. Since the solution of Eq. (18) can be cast in the form,

$$\psi_i(\mathbf{q}, s) = \sum_r \mathcal{Q}_{ir} \psi_r(\mathbf{q}, 0), \quad (31)$$

where $\mathcal{Q} = \mathbf{A}^{-1}\mathbf{B}$, the correlation functions of the form $\langle \psi_i(\mathbf{q}, s) \psi_j(-\mathbf{q}, 0) \rangle$ follow as

$$\langle \psi_i(\mathbf{q}, s) \psi_j(-\mathbf{q}, 0) \rangle = \sum_r \mathcal{Q}_{ir} \langle \psi_r(\mathbf{q}, 0) \psi_j(-\mathbf{q}, 0) \rangle, \quad (32)$$

where the equal-time correlation functions, which follow from the thermodynamic theory of fluctuations, read

$$\langle |\psi_1(\mathbf{q}, 0)|^2 \rangle = \frac{V^2}{N_0} \frac{(\gamma - 1)}{\gamma}, \quad (33)$$

$$\langle |\psi_2(\mathbf{q}, 0)|^2 \rangle = \frac{V^2}{N_0} x_1 x_2 \frac{(m_1 m_2)^2}{(m_1 x_1 + m_2 x_2)^4}, \quad (34)$$

$$\langle |\psi_3(\mathbf{q}, 0)|^2 \rangle = \frac{V^2}{N_0} \gamma, \quad (35)$$

where N_0 is the total number of molecules in the volume V of the scattering region. In terms of the set of dimensionless variables (ψ_1 , ψ_2 , ψ_3) we can now write the dynamic structure factor of Eq. (2) as

$$S(\mathbf{q}, \omega) = 2 \sum_{ij} \left(\frac{\partial \epsilon}{\partial \psi_i} \right) \left(\frac{\partial \epsilon}{\partial \psi_j} \right) \langle |\psi_j(\mathbf{q}, 0)|^2 \rangle \text{Re}[\mathcal{Q}_{ij}(s = i\omega)]. \quad (36)$$

Note that the matrix element containing ψ_4 needs not be evaluated since it does not appear in the structure factor $S(\mathbf{q}, \omega)$. For a binary mixture obeying the Clausius-Mossotti relation (see, for example, the textbook of Born [28]) we can obtain the following relations:

$$\left(\frac{\partial \epsilon}{\partial \psi_1} \right) = -\frac{N_0}{V} (\alpha_1 x_1 + \alpha_2 x_2), \quad (37)$$

$$\left(\frac{\partial \epsilon}{\partial \psi_2} \right) = \frac{N_0}{V} \frac{(m_1 x_1 + m_2 x_2)^2}{m_1 m_2} (\alpha_1 - \alpha_2), \quad (38)$$

$$\left(\frac{\partial \epsilon}{\partial \psi_3} \right) = \frac{N_0}{V} \frac{1}{\gamma} (\alpha_1 x_1 + \alpha_2 x_2), \quad (39)$$

in which α_1 , α_2 are the dynamic polarizabilities of the two molecular species at the frequency of the incident light. The molecular polarizabilities at 532.22 nm can be found in Table I.

This model is tightly related to the transport coefficients of the binary mixture: the bulk viscosity η_b , the shear viscosity $\eta_s = [\eta_s]_1 + [\eta_s]_2$, the thermal conductivity λ_{th} , the diffusion coefficient D_{12} , and the thermal diffusion ratio k_T . The characteristic relaxation times and the usual transport coefficients appearing in the generalized constitutive relations of Eqs. (11)–(13) are given by

$$\eta_b = \frac{3}{2} (\gamma - 1) (5/3 - \gamma) p \tau_v, \quad (40)$$

$$[\eta_s]_1 = \frac{5}{8} \frac{x_1 k_B T}{x_1 \Omega_{11}^{(2,2)} + 2x_2 \Omega_{12}^{(2,2)}}, \quad (41)$$

$$[\eta_s]_2 = p x_2 \tau_2 = \frac{5}{8} \frac{k_B T}{\Omega_{22}^{(2,2)}}, \quad (42)$$

$$D_{12} = k_B T \frac{m_1 x_1 + m_2 x_2}{m_1 m_2} \tau_w = \frac{3}{16} \frac{(k_B T)^2 (m_1 + m_2)}{p m_1 m_2 \Omega_{12}^{(1,1)}}, \quad (43)$$

$$D_{11} = \frac{3}{8} \frac{(k_B T)^2}{p m_1 \Omega_{11}^{(1,1)}}, \quad (44)$$

$$D_{22} = \frac{3}{8} \frac{(k_B T)^2}{p m_2 \Omega_{22}^{(1,1)}}, \quad (45)$$

$$[\lambda_{\text{th}}]_1 = \frac{75 k_B}{32 m_1 x_1 \Omega_{11}^{(2,2)} + x_2 \left(\frac{25}{2} \Omega_{12}^{(1,1)} - 10 \Omega_{12}^{(1,2)} + 2 \Omega_{12}^{(1,3)} \right)} + \frac{\rho_1 [c_v^{\text{int}}]_1}{x_1/D_{11} + x_2/D_{12}}, \quad (46)$$

$$[\lambda_{\text{th}}^{\text{tr}}]_2 = \frac{5 k_B}{2 m_2} p x_2 \tau_2' = \frac{75 k_B}{32 m_2} \frac{k_B T}{\Omega_{22}^{(2,2)}}, \quad (47)$$

$$[\lambda_{\text{th}}^{\text{int}}]_2 = p [c_v^{\text{int}}]_2 x_2 \tau_2'' = \frac{\rho_2 [c_v^{\text{int}}]_2}{x_1/D_{12} + x_2/D_{22}}, \quad (48)$$

$$k_T = \frac{5}{2} x_1 x_2 \frac{m_1 m_2}{(m_1 x_1 + m_2 x_2)^2} \times \frac{(5 \Omega_{12}^{(1,1)} - 2 \Omega_{12}^{(1,2)})}{x_1 \Omega_{11}^{(2,2)} + x_2 \left(\frac{25}{2} \Omega_{12}^{(1,1)} - 10 \Omega_{12}^{(1,2)} + 2 \Omega_{12}^{(1,3)} \right)}, \quad (49)$$

$$k_p = p \frac{(\partial \mu / \partial p)_{c,T}}{(\partial \mu / \partial c)_{p,T}} = x_1 x_2 (m_2 - m_1) \frac{m_1 m_2}{(m_1 x_1 + m_2 x_2)^3}, \quad (50)$$

$$\left(\frac{\partial \mu}{\partial c} \right)_{p,T} = \frac{k_B T}{x_1 x_2} \frac{(m_1 x_1 + m_2 x_2)^3}{(m_1 m_2)^2}, \quad (51)$$

where

$$[c_v^{\text{int}}]_i = \frac{3}{2} \frac{(5/3 - \gamma_i) k_B}{(\gamma_i - 1) m_i} \quad (52)$$

is the isochoric specific heat capacity associated with the internal degrees of freedom of molecules of the i component and $\Omega_{ij}^{(l,r)}$ denotes the elastic Chapman-Cowling collision integrals [35].

Since collision integrals can only be evaluated for a specific interaction between molecules, we shall consider in this paper the Lennard-Jones (6-12) potential function:

$$U_{ij}(r) = 4\epsilon_{ij} \left[\left(\frac{\sigma_{ij}}{r} \right)^{12} - \left(\frac{\sigma_{ij}}{r} \right)^6 \right], \quad (53)$$

where r is the distance between the centers of mass of the two molecules, ϵ_{ij} the maximum depth of the potential well, and σ_{ij} is the distance at which the potential function vanishes. The values of the Lennard-Jones potential parameters (σ_{ij} and ϵ_{ij}) adopted in this model are extracted from literature and listed in Table II. The elastic collision integrals $\Omega_{ij}^{(l,r)}$ are expressed as

$$\Omega_{ij}^{(l,r)} = \sigma_{ij}^2 \sqrt{\frac{2\pi k_B T}{m_{ij}}} \frac{(r+1)!}{4} \left[1 - \frac{1}{2} \frac{(1+(-1)^l)}{1+l} \right] \Omega_{ij}^{*(l,r)}, \quad (54)$$

where $m_{ij} = m_i m_j / (m_i + m_j)$ is the reduced mass, and $\Omega_{ij}^{*(l,r)}$ are the reduced collision integrals [38], which are functions of the reduced temperature $T^* = k_B T / \epsilon_{ij}$.

A substantial simplification of our model can be achieved if we consider a mixture of Maxwellian molecules, for which

TABLE II. Parameters for the Lennard-Jones potentials σ_{ij} and ϵ_{ij} for binary gases.

	σ_{ij} (nm)			
	SF ₆	He	D ₂	H ₂
SF ₆	0.5252 ^a	0.4298 ^a	0.4420 ^c	0.4396 ^c
He		0.2576 ^b		
D ₂			0.2948 ^b	
H ₂				0.2968 ^b
	ϵ_{ij}/k_B (K)			
	SF ₆	He	D ₂	H ₂
SF ₆	207.7 ^a	19.24 ^a	42.65 ^c	39.77 ^c
He		10.12 ^b		
D ₂			39.3 ^b	
H ₂				33 ^b

^aReference [36].

^bReference [15].

^cCalculated based on the Kong rule [37].

thermal diffusion is automatically absent. However, Letamendia and co-workers [15] have shown that the light scattering spectrum in disparate-mass gas mixtures is very sensitive to the presence and magnitude of thermal-diffusion effects. An estimate of the contribution of thermal-diffusion effects to the spectral shape was presented by Johnson [39], who showed that thermal-diffusion effects are comparable in magnitude to other first-order dissipative contributions (heavy-species heat flux and viscosity) in disparate-mass gas mixtures

Lastly, we close this section by remarking that the calculation of the spectral distribution of scattered light for a disparate-mass gas mixture can be calculated from the dynamic structure factor $S(\mathbf{q}, \omega)$, which was defined in Eq. (2), and further evaluated in the present framework to Eq. (36) under the crucial assumption that m_1/m_2 is small. It requires the specification of the molecular masses, polarizabilities, specific heat capacity ratios for all constituents, and Lennard-Jones potential parameters for all combinations of species. Based on these quantities we can determine (i) the transport coefficients (41)–(51) and (ii) the relaxation times τ_2 , τ_2' , τ_2'' , τ_w , and τ_s . Thus, the only free adjustable parameter of our generalized hydrodynamic description is the relaxation time τ_v , which is connected to the bulk viscosity of the binary mixture via Eq. (40). Since this is a quantity which cannot be computed within the current framework, we define the so-called internal relaxation number $z = \tau_v/\tau_s$ representing the ratio between the mean elastic and inelastic molecular collision frequencies. The value of z can then be determined for each binary mixture from the experimental input. Through the known value of $\tau_s = \eta_s/p$, the stress relaxation time setting the unit of time, the z parameter is equivalent to

$$z = \frac{\eta_b}{\eta_s} \frac{2}{(\gamma - 1)(5 - 3\gamma)}. \quad (55)$$

A similar, but simplified, derivation of the dynamic structure factor $S(\mathbf{q}, \omega)$ can be performed within the framework of classical hydrodynamics, starting from the same matrix equation Eq. (18). In this case the matrix elements containing

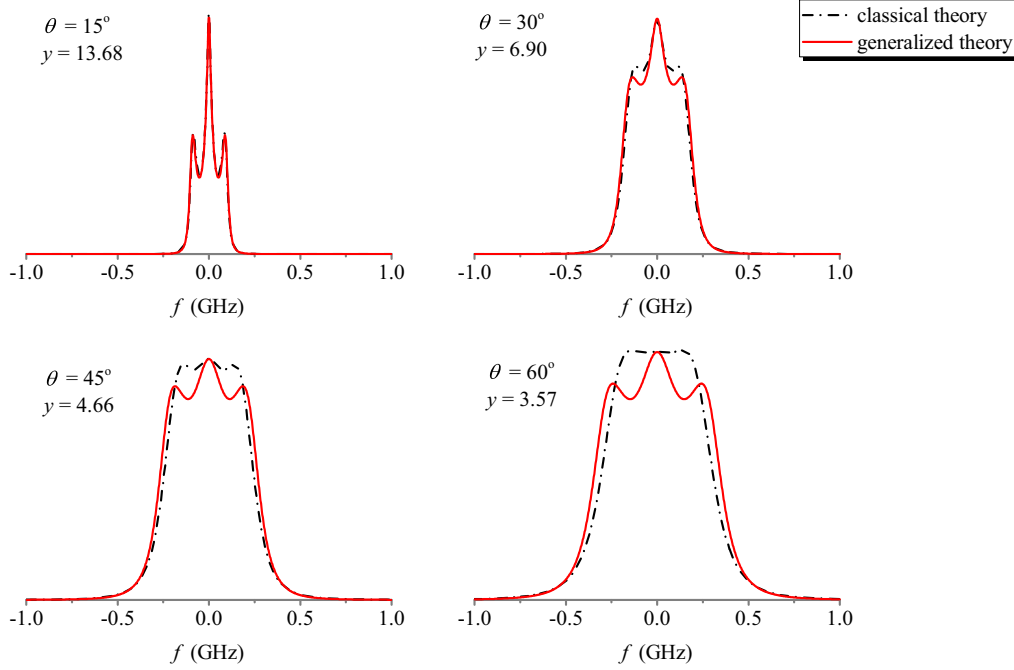


FIG. 1. Comparison of computations of the RB-scattering profiles between generalized macroscopic theory vs classical hydrodynamics approach for mixtures with internal relaxation number $z = 10$ for varying scattering angles θ and the case of $p = 1$ bar SF_6 in a mixture with $p = 1$ bar of helium.

the functional forms $g(s)$, $f(s)$, and $b(s)$ are then replaced by the expressions in Eqs. (28)–(30). Rayleigh-Brillouin spectra are computed and a comparison is made with the spectra computed from the complex relaxation hydrodynamics model. A comparison is made for a collisional number of $z = 10$ in both cases, but for a variety of scattering angles θ . This value of $z = 10$ approximately corresponds to the condition of $p = 1$ bar of SF_6 combined with $p = 1$ bar of helium, for conditions $T = 295$ K and $\lambda_i = 532$ nm (see below).

The variation of θ is included in the computations to illustrate the transition from the kinetic to the hydrodynamic regime. The uniformity parameter for the mixture equals

$$y = \frac{\lambda_i/n}{4\pi \sin \theta/2} \frac{p}{\eta_s \sqrt{2k_B T/m}}, \quad (56)$$

where p is the total pressure and the mass m is to be taken as the mean in the mixture $m = x_1 m_1 + x_2 m_2$. This representation of y involves an explicit dependence on the scattering angle θ , while all other parameters are kept constant in the comparisons shown in Fig. 1. As indicated, for small scattering angles, hence in the hydrodynamic regime, both theories match closely. Note that $\theta = 15^\circ$ corresponds to $y = 13.68$. However, in the kinetic regime of lower values of the uniformity parameter, at $\theta = 60^\circ$ corresponding to $y = 3.57$, strong deviations are found.

III. EXPERIMENTAL SETUP

The experimental setup used for measuring spontaneous Rayleigh-Brillouin scattering at a wavelength of 532.22 nm, shown in Fig. 2, has been described previously [11]. The light from a frequency-doubled Nd:VO₄ laser (Coherent, Verdi-5), at a power of 5 Watt and bandwidth less than 5 MHz travels

through the binary gas medium. For the scattering cell, two Brewster-angled windows are mounted at entrance and exit ports to reduce stray light. A pressure gauge is connected to the cell to monitor the pressure and a temperature control system involving PT-100 sensors, Peltier elements as well as water cooling are used to keep the cell at a constant temperature with uncertainty less than 0.1 °C. The laser wavelength is monitored by a wavelength meter (Toptica HighFinesse WSU-30).

The scattered light propagates through a bandpass filter (Materion, $T > 90\%$ at $\lambda_i = 532$ nm, bandwidth $\Delta\lambda = 2.0$ nm) onto a Fabry-Perot interferometer (FPI) with an effective free spectral range (FSR) of 2.9964(5) GHz and an instrument width of $\sigma_{\text{instr}} = 58.0 \pm 3.0$ MHz (FWHM). The calibration methods were discussed by Gu *et al.* [40]. The instrument function is verified to exhibit the functional form of an Airy function, which may be well approximated by a Lorentzian function during data analysis.

For the present experiments a scattering angle $\theta = 55.7 \pm 0.3^\circ$ is adopted, because at angles smaller than the usual setting of $\theta = 90^\circ$ the Brillouin side peaks become more pronounced [20,21]. The angle was determined by a homemade rotation goniometer stage, while the opening angle is less than 0.5° , calculated from the geometry of a slit set behind the gas cell at a certain distance from the scattering center.

RB-scattering spectral profiles were recorded by piezo-scanning the FPI at integration times of 1 s for each step, usually over 18 MHz, with detection of the scattered light on a photomultiplier (PMT) after the FPI analyzer. A full spectrum covering many consecutive RB peaks and 10 000 data points was obtained in about 3 h. The piezo-voltage scans were linearized and converted to frequency scale by fitting the RB-peak separations to the calibrated FSR value. The

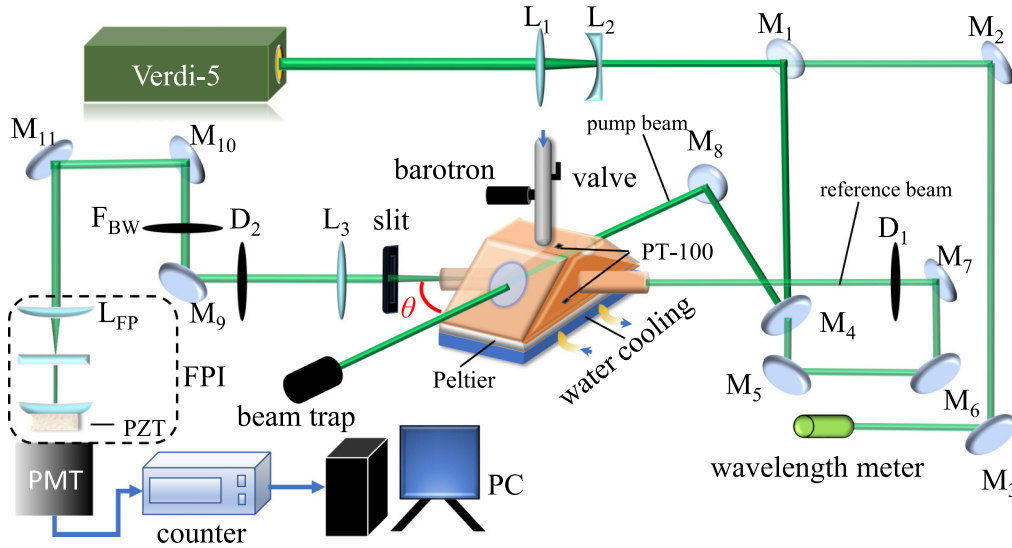


FIG. 2. Schematic diagram of the experimental setup for spontaneous Rayleigh-Brillouin scattering at 532 nm. A Verdi-V5 laser provides continuous wave light at 532.22 nm, at a power of 5 Watt and bandwidth less than 5 MHz. The laser light is split into two beams. The pump beam crosses the RB-scattering gas cell producing scattered light that is captured under an angle $\theta = (55.7 \pm 0.3)^\circ$. A small fraction of the power, retained in a reference beam transmitted through M_4 , is used to align the beam path after the gas cell towards the detector. The scattered light after a bandpass filter (F_{BW}) is analyzed in a Fabry-Perot interferometer (FPI), with free spectral range of 2.9964 GHz and an instrument linewidth of (58 ± 3) MHz, and is collected on a photo-multiplier tube (PMT). Mirrors, lenses, and diaphragm pinholes are indicated as M_i , L_i , and D_i . A slit of $500 \mu\text{m}$ is inserted to limit the opening angle for collecting scattering light, therewith optimizing the resolution.

methods for producing such concatenated RB spectra have been detailed before [40,41].

IV. RESULTS AND COMPARISON

Rayleigh-Brillouin light scattering spectra were measured for gas mixtures consisting of SF_6 , the heaviest molecular species to be put in the gas phase at high pressures, combined with gases of the lightest molecules available. Molecular hydrogen (H_2) and its isotopologue deuterium (D_2) exhibit the same physical and chemical properties, and only the masses are different at 2 amu and 4 amu. As for a comparison with helium, its mass is the same as that of D_2 , while the attractive potential depth for interactions with SF_6 is much smaller. These combinations provide an interesting test ground for verifying the relaxation hydrodynamic model put forward in Sec. II. Foremost, the combination of SF_6 with low-mass admixed gas fulfills the condition of disparate masses, $m_1 < m_2$. The experimental conditions are chosen keeping a standard pressure of 1 bar SF_6 , mixed with gases of the lighter species, at pressures stepwise increasing from 0.5 bar to 4 bar. A list

of all pressure combinations experimentally investigated is provided in Table III. All measurements were performed at room temperature, at $\lambda = 532.22 \text{ nm}$ and $\theta = 55.7^\circ$.

The measured RB light scattering spectra, shown in Fig. 3 for mixtures with He, in Fig. 4 for mixtures with D_2 , and in Fig. 5 for mixtures with H_2 , all show the same qualitative behavior. In general terms the light scattering of the binary mixtures under investigation is fully dominated by the SF_6 molecules. The polarizability of SF_6 is extremely large, causing this molecule to exhibit a very large Rayleigh cross section [42]. In relative terms the polarizability, and therewith the cross section for the light collisional partners is very small, such that these in fact only behave as “spectators,” an effect that was also observed for Ar/He and Kr/He mixtures [19], although not as pronounced as in the present case.

While for single-component gases the Brillouin side peaks become more pronounced when increasing the gas pressure, such as was observed for pure SF_6 gas [43], for CO_2 [11], and for N_2O [12] in the present case with increasing pressure of the collisional partner in a mixture, the reverse is true. The addition of light-mass constituents to the gas causes the

TABLE III. The conditions of mixture gases experimentally investigated and the fitting result of the internal relaxation number z .

SF_6 He		SF_6 D_2			SF_6 H_2					
p (bar)	T (K)	z	p (bar)	T (K)	z	p (bar)	T (K)	z		
1.032	295.0		1.007	293.2		1.002	293.2			
1.033	0.512	18.73(0.83)	1.001	0.506	293.2	16.68(0.38)	1.002	0.510	293.2	20.75(0.56)
1.037	1.029	9.74(0.36)	1.002	1.001	293.2	9.91(0.13)	1.002	1.004	293.2	13.06(0.20)
1.037	2.146	2.44(0.49)	1.002	2.003	293.2	2.67(0.13)	1.002	2.007	293.2	5.28(0.06)
1.035	2.993	0.30(0.08)	1.002	3.002	293.2	1.40(0.07)	1.002	3.002	293.2	2.51(0.33)
1.037	4.084	< 0.1	1.002	4.002	293.2	1.64(0.12)	1.004	4.001	293.2	1.83(0.12)

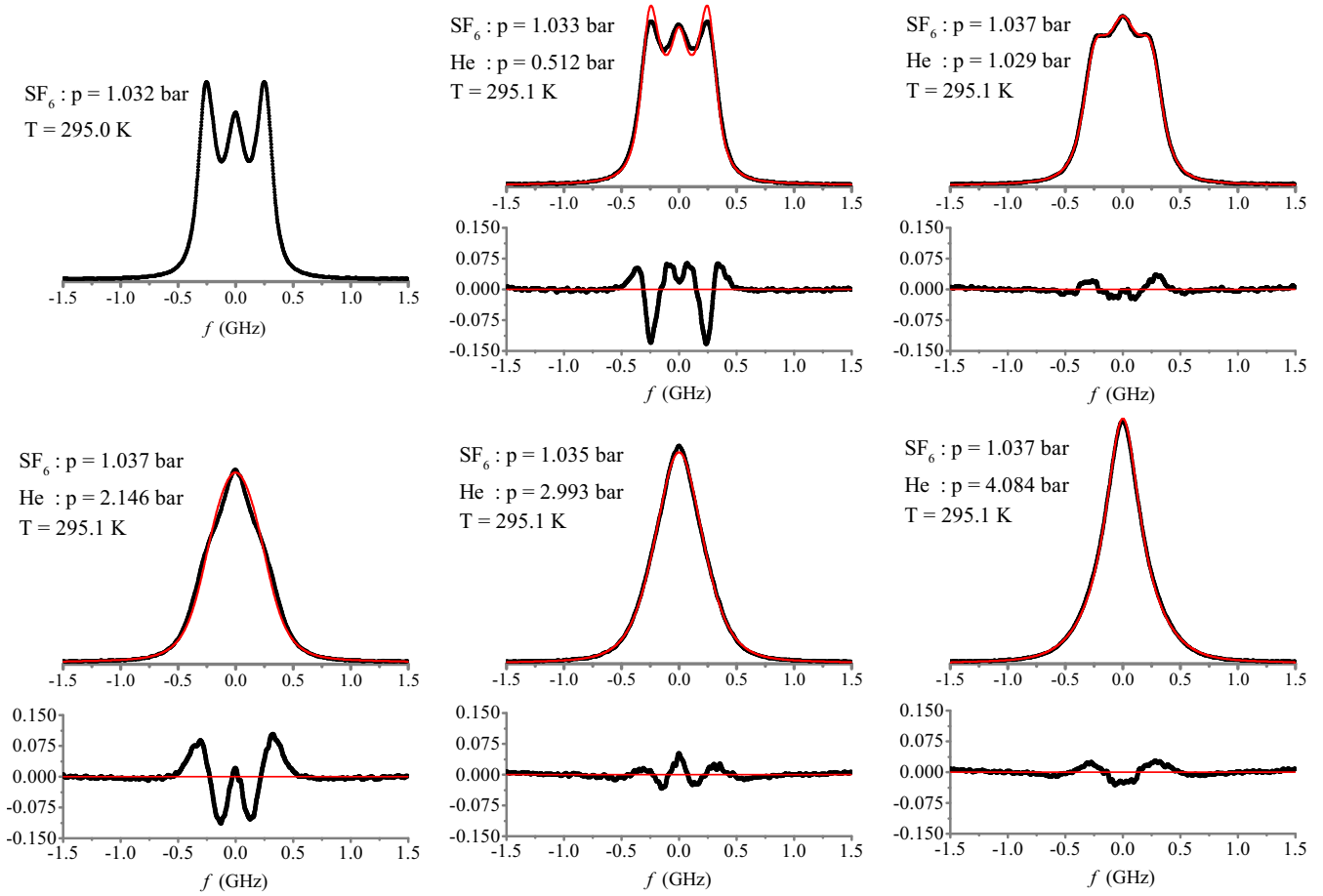


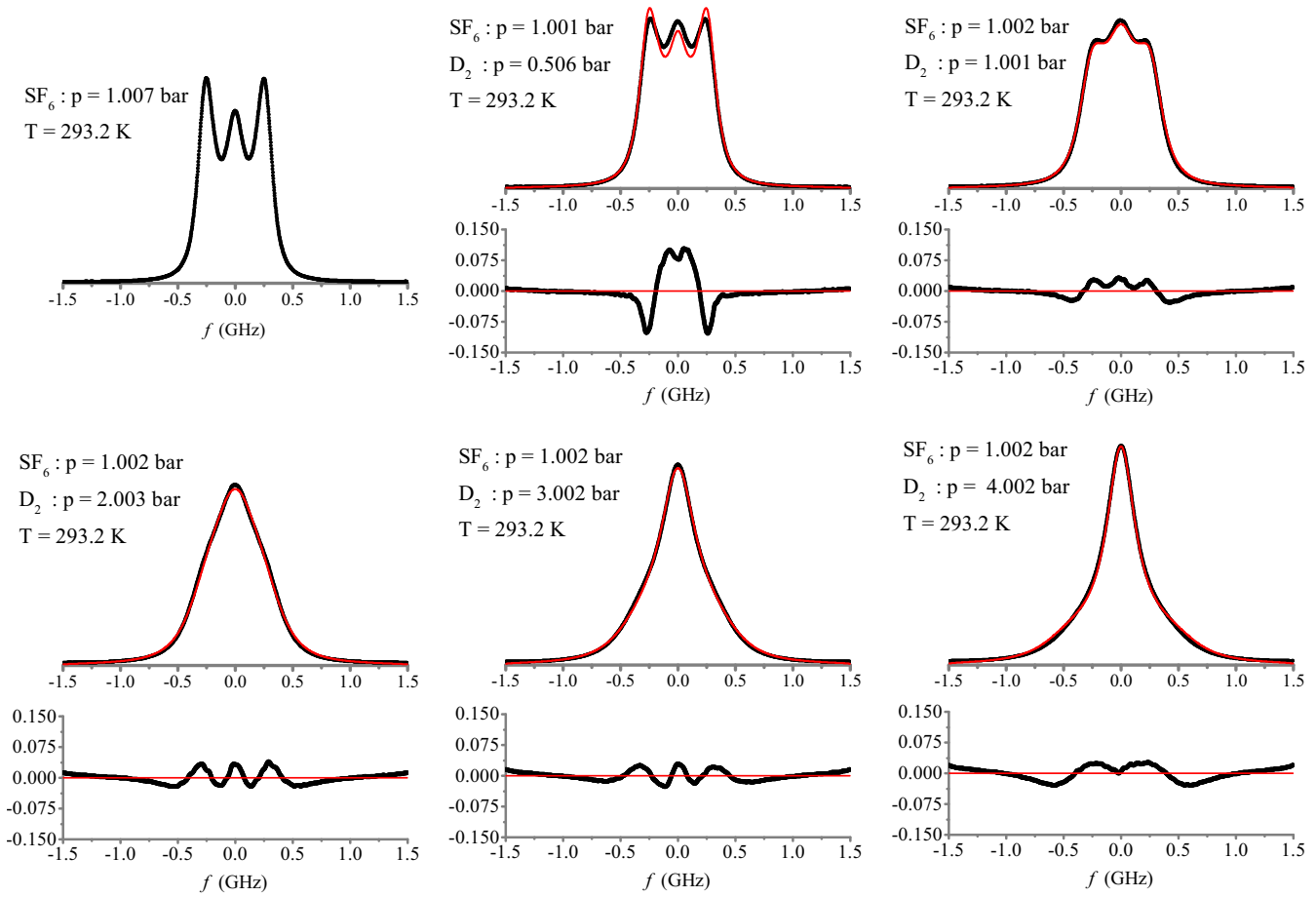
FIG. 3. Measured Rayleigh-Brillouin scattering profiles (black) of binary mixtures of SF₆-He as measured for the various conditions as indicated, and a comparison with the binary mixture model (red). Also an RBS spectrum of pure SF₆, at 1 bar, is shown for comparison. Bottom graphs display the corresponding residuals. The experimental data were measured at wavelength of $\lambda_i = 532.22$ nm and scattering angle of $\theta = 55.7^\circ$, and these spectra are on a scale of normalized integrated intensity over one FSR.

RBS profile to exhibit less pronounced Brillouin side peaks. A comparison with the profile measured for 1 bar of pure SF₆, as shown in the figures, demonstrates this; for the pure SF₆ gas the side peaks are most pronounced. A further effect of the addition of light-mass collision partners is the narrowing of the composite RBS profile for increased pressures, and for all three collision partners alike. So, even though the light collision partners do not contribute to the light scattering themselves, their influence as collision partner is decisive in framing the light scattering spectrum.

The experimentally measured RB spectra for the various gas mixtures are compared to spectra computed with the theoretical model for binary gas mixtures as described in Sec. II. The dynamic structure function $S(\mathbf{q}, \omega)$ is calculated with input from known properties of the SF₆ molecule and the light collision partner, which is basically the dynamic polarizability α , the heat capacity ratio γ , the coefficients $\epsilon_{i,j}$ and $\sigma_{i,j}$ that define the intermolecular interactions via the Lennard-Jones potential. All gas-transport coefficients needed to evaluate the $S(\mathbf{q}, \omega)$ function are then defined, with the exception of the bulk viscosity of the system, which was parametrized via a single value of z in Eq. (55). Extensive computations were performed in which z was treated as a fitting parameter for

each individual case of binary mixture in a least squares analysis. The computed spectra for the optimized values of z are plotted in Figs. 3–5, where also residuals between theory and experiment are presented. A general trend can be discerned from the comparison between experimental and theoretical spectra. The largest discrepancies occur for the lowest pressure of additions of 0.5 bar of the lighter component, with residuals exhibiting extrema of some 10% and 15% for H₂. The agreement overall improves for the largest additions of the low-mass scattering partners, where deviations decrease to 2%–3%.

The computations and fitting procedures lead to a set of values for the z parameter, the collisional number for reaching thermal equilibrium between translational and internal energies in the binary mixtures. Results for all combinations of heavy and light species are displayed in Fig. 6, while z values and uncertainties are also listed in Table III. During the fitting optimization of the z parameter it was found that the computed spectra were found to sensitively depend on the values for the heat capacity ratio of $\gamma(\text{SF}_6)$. In these procedures we adopted the experimental value from literature and kept fixed at $\gamma = 1.10$ [33]. Also the γ values for the light collision partners were set to the literature values as listed in Table I.

FIG. 4. Same as Fig. 3 now for SF₆/D₂ mixtures.

It is noted, that for an optimized value of $\gamma(\text{SF}_6) = 1.13$, with some differences for various cases of pressures and low-mass mixing partners, a near to perfect match is found between experiment and the generalized RB-scattering theory. This may indicate that the latter is a better value for the the heat capacity ratio, and that the present approach constitutes a manner to determine heat capacity ratios. However, the strong correlations between parameters z and $\gamma(\text{SF}_6)$ in the fitting procedures would require further investigations.

The so-called internal relaxation number $z = \tau_v/\tau_s$ characterizes the ratio between elastic and inelastic molecular collision frequencies. As a rule, inelastic collisions—that describe the transfer of energy between translational and internal degrees of freedom—occur less frequently than elastic collisions. In particular, if the molar fraction of the light constituent increases in a disparate-mass gas mixture, the mean number of inelastic collisions per unit of time suffered by both constituents increases and leads to a decrease of the internal relaxation number. Based on kinetic gas theory [44], it may be verified that in a binary mixture of polyatomic gases the bulk viscosity η_b of the mixture decreases as the molar fraction of the light constituent increases. Since the parameter z is proportional to the bulk viscosity of the gas mixture, this fact could also explain the decrease of the internal relaxation number as we add light constituents to the mixture.

The trends for the z parameter only show slight differences for the three different collision partners of low mass, but in view of the small uncertainties as resulting from the fitting procedures (cf. Fig. 6), these small differences are significant. In case of H₂ as the collision partner the value of z is somewhat larger at a certain pressure, which is indicative of the fact that the heavier species of He and D₂ lead to more efficient relaxation. It should be noted that the generalized hydrodynamic model approach, presented here, makes the assumption that the masses of heavy and light scatterers are strongly disparate, but the mass of the light collision partners does not enter in the model description. So, in view of the fact that the Lennard-Jones coefficients for collisions between SF₆ with H₂ or D₂ are very similar (cf. Table II), no difference between H₂ and D₂ as collision partner would be expected. While Fig. 6 compares the resulting values of z , in Fig. 7 the observed spectra for collision with 1 bar of the light species are compared. This shows that there is an observable difference for H₂ and D₂ as collision partners, an effect that goes beyond the current model description. The fact that the RB spectra with colliding He and D₂ (at 1 bar admixture) are overlapping, leads to the same z parameter for these conditions as shown in Fig. 6. The latter correspondence of z value for He and D₂ is indicative of the fact that the specific characteristics of the molecular interaction, as in the ϵ_{ij} and σ_{ij} Lennard-Jones parameters, only plays a marginal role. Only at the highest pressures

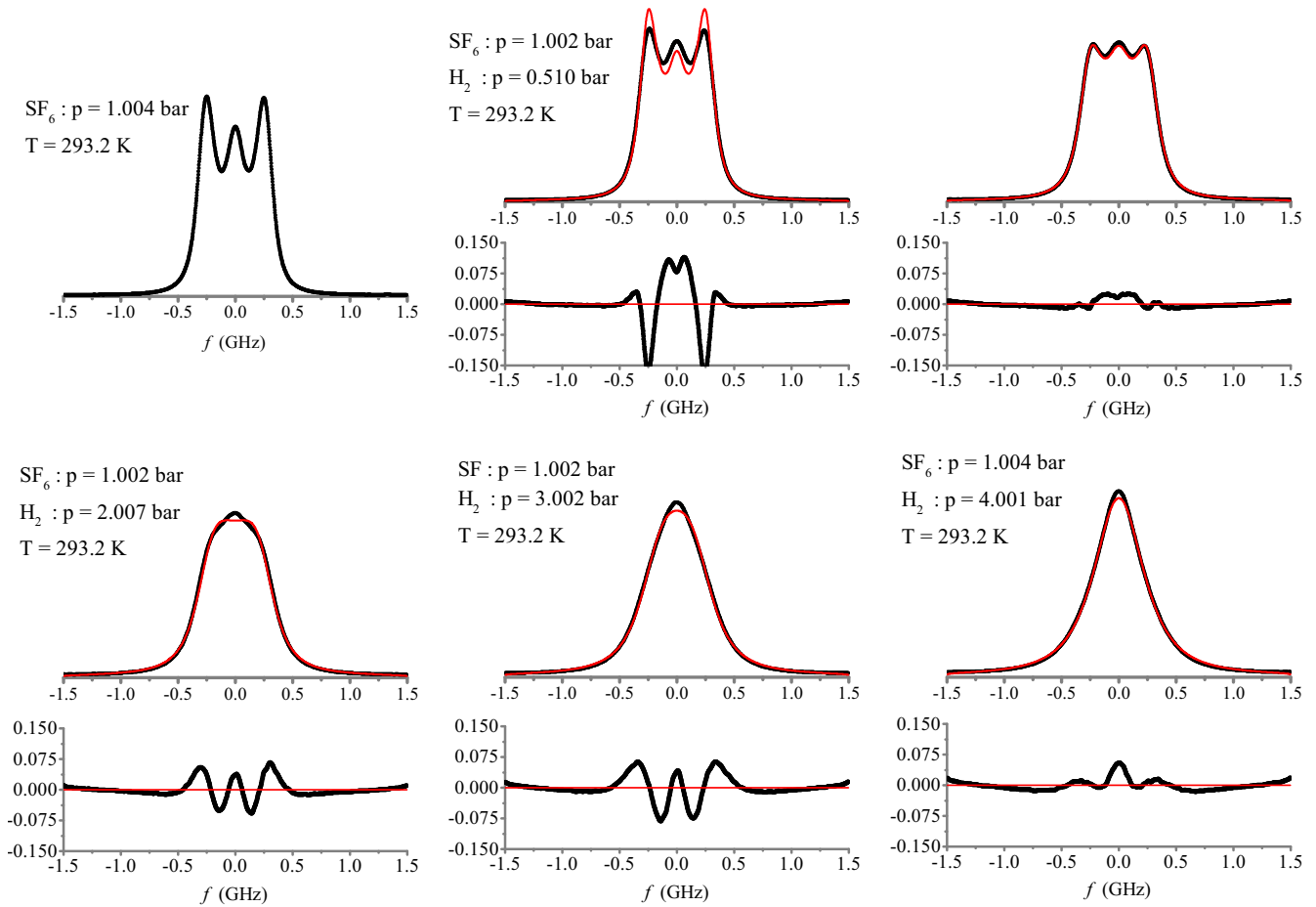


FIG. 5. Same as Fig. 3 now for SF₆/H₂ mixtures.

there arises a deviation between He and D₂ as collision partners.

Finally, for an explicit comparison between the observed RBS profiles and the results from the two theories, general-

ized relaxation hydrodynamics and classical hydrodynamics, results are plotted in Fig. 8 for the specific case of a 1:1 mixture of SF₆/He at $p = 2$ bar. This example shows that the generalized theory gives a superior description of the obtained experimental results, in particular where the kinetic regime is entered in the case of smaller value of y .

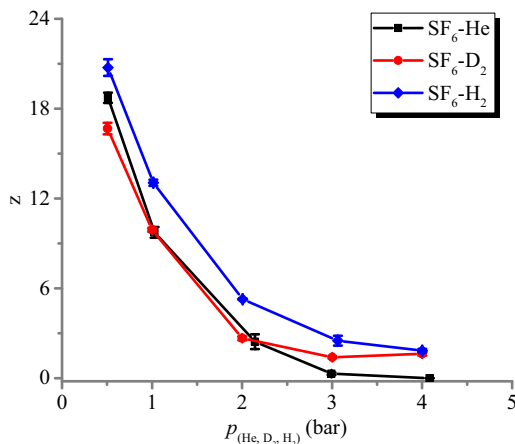


FIG. 6. The value of z derived from the comparison between experimental spectra and computed spectra for generalized hydrodynamics, for all pressure combinations, and for the three mixtures of SF₆-He, SF₆-D₂, and SF₆-H₂. The derived uncertainties are also indicated.

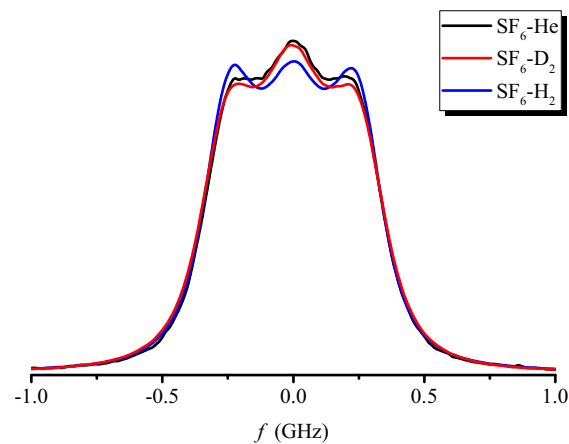


FIG. 7. Direct comparison of experimental Rayleigh-Brillouin scattering profiles for 1 bar SF₆, admixed with 1 bar of the three light collision partners He, H₂, and D₂.

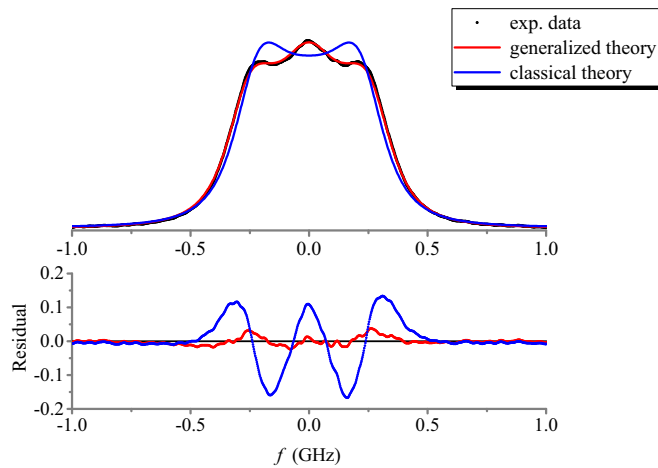


FIG. 8. Comparisons between the measured Rayleigh-Brillouin scattering profiles of binary mixtures of SF_6 -He and generalized relaxation hydrodynamics theory as well as for the classical hydrodynamics approach for mixtures. The experimental data were measured with 1 bar SF_6 and 1 bar He at wavelength of $\lambda_i = 532.22$ nm and scattering angle of $\theta = 55.7^\circ$. The theoretical spectra are, for the purpose of comparison with experiment, convolved with the instrumental width of 58 MHz. The spectra are plotted on a scale of normalized integrated intensity over one FSR.

V. CONCLUSION

A relaxation hydrodynamical model for binary mixture gases is developed that is based on the assumption that the masses of collision partners are disparate. In the model description all macroscopic transport coefficients are computed from the molecular interactions between heavy-heavy, heavy-light, and light-light species from a Lennard-Jones potential by invoking the well-tested two-parameter components for the potentials: well depth and characteristic range. Further, the heat capacity ratios $\gamma = c_p/c_v$ and the dynamic polarizabilities α for the gas components are used. From these inputs, the entire collisional model is produced that allows for

a computation of the dynamic structure factor $S(\mathbf{q}, \omega)$ which is representative of the Rayleigh-Brillouin light scattering spectrum. However, a single ingredient is lacking to complete the calculations: an overall relaxation parameter which can be associated with the bulk viscosity of the binary mixture. This is subsequently set as a fitting parameter in the description of light scattering of binary mixtures.

The model is experimentally tested by performing measurements on binary mixture gases that fulfill the assumption of disparate masses nearly perfectly. For the heavy component, the gas with the heaviest molecular species is chosen that can be brought in the gas phase at high pressure: hexafluoride (SF_6). This is combined with the lightest collision partners available, helium gas and hydrogen gas, the latter for two isotopologues H_2 and D_2 . Incidentally the polarizability of the light scattering partners is so small, with respect to that of SF_6 that they behave only as spectators in the light scattering process; the light scattered by the light species is negligible for the spectrum. Nevertheless the activity of the light species as collision partners decisively alters the spectra profiles. The Brillouin side peaks in the RB profiles, which are known to become more pronounced at increasing pressure for single species gases, become strongly damped and disappear gradually with higher mole fractions of helium and hydrogen added.

As for a final conclusion the presently developed generalized relaxation hydrodynamics model for Rayleigh-Brillouin scattering in binary gases, based on an assumption of mass-disparate constituents in the gas, provides a good representation of experimentally observed spectral profiles for heavy SF_6 in mixtures with light He, D_2 , and H_2 . Also the model is shown to be superior to a description in terms of classical hydrodynamics.

ACKNOWLEDGMENT

Y.W. acknowledges support from the Chinese Scholarship Council (CSC) for his stay at VU Amsterdam.

- [1] R. B. Miles, W. R. Lempert, and J. N. Forkey, Laser Rayleigh scattering, *Meas. Sci. Technol.* **12**, R33 (2001).
- [2] T. A. Mcmanus, I. T. Monje, and J. A. Sutton, Experimental assessment of the Tenti S6 model for combustion-relevant gases and filtered Rayleigh scattering applications, *Appl. Phys. B* **125**, 13 (2019).
- [3] D. Bruno, Direct simulation Monte Carlo simulation of thermal fluctuations in gases, *Phys. Fluids* **31**, 047105 (2019).
- [4] S. Yip and M. Nelkin, Application of a kinetic model to time-dependent density correlations in fluids, *Phys. Rev.* **135**, A1241 (1964).
- [5] R. D. Mountain, Spectral distribution of scattered light in a simple fluid, *Rev. Mod. Phys.* **38**, 205 (1966).
- [6] W. Marques Jr. and G. M. Kremer, Light scattering from extended kinetic models: Monatomic ideal gases, *Continuum Mech. Thermodyn.* **10**, 319 (1998).
- [7] C. D. Boley, R. C. Desai, and G. Tenti, Kinetic models and Brillouin scattering in a molecular gas, *Can. J. Phys.* **50**, 2158 (1972).
- [8] G. Tenti, C. D. Boley, and R. C. Desai, On the kinetic model description of Rayleigh-Brillouin scattering from molecular gases, *Can. J. Phys.* **52**, 285 (1974).
- [9] Z. Gu and W. Ubachs, Temperature-dependent bulk viscosity of nitrogen gas determined from spontaneous Rayleigh-Brillouin scattering, *Opt. Lett.* **38**, 1110 (2013).
- [10] Z. Gu, W. Ubachs, and W. van de Water, Rayleigh-Brillouin scattering of carbon dioxide, *Opt. Lett.* **39**, 3301 (2014).
- [11] Y. Wang, W. Ubachs, and W. van de Water, Bulk viscosity of CO_2 from Rayleigh-Brillouin light scattering spectroscopy at 532 nm, *J. Chem. Phys.* **150**, 154502 (2019).
- [12] Y. Wang, K. Liang, W. van de Water, W. Marques, and W. Ubachs, Rayleigh-Brillouin light scattering spectroscopy of nitrous oxide (N_2O), *J. Quant. Spectrosc. Radiat. Transfer* **206**, 63 (2018).
- [13] R. D. Mountain and J. Deutch, Light scattering from binary solutions, *J. Chem. Phys.* **50**, 1103 (1969).

- [14] C. Cohen, J. Sutherland, and J. Deutch, Hydrodynamic correlation functions for binary mixtures, *Phys. Chem. Liq.* **2**, 213 (1971).
- [15] L. Letamendia, J. P. Chabrat, G. Nouchi, J. Rouch, C. Vaucamps, and S. H. Chen, Light-scattering studies of moderately dense gas mixtures. Hydrodynamic regime, *Phys. Rev. A* **24**, 1574 (1981).
- [16] L. Letamendia, G. Nouchi, and S. Yip, Kinetic model of the generalized Enskog equation for binary mixtures, *Phys. Rev. A* **32**, 1082 (1985).
- [17] C. D. Boley and S. Yip, Modeling theory of the linearized collision operator for a gas mixture, *Phys. Fluids* **15**, 1424 (1972).
- [18] J. R. Bonatto and W. Marques Jr., Kinetic model analysis of light scattering in binary mixtures of monatomic ideal gases, *J. Stat. Mech.* (2005) P09014.
- [19] Z. Gu, W. Ubachs, W. Marques, and W. van de Water, Rayleigh-Brillouin Scattering in Binary-Gas Mixtures, *Phys. Rev. Lett.* **114**, 243902 (2015).
- [20] I. L. Fabelinskii, *Molecular Scattering of Light* (Springer Science, Heidelberg, 2012).
- [21] Y. Wang, Z. Gu, K. Liang, and W. Ubachs, Rayleigh-brillouin light scattering spectroscopy of air; Experiment, predictive model and dimensionless scaling, *Mol. Phys.*, e1804635 (2020).
- [22] S. R. de Groot and P. Mazur, *Non-Equilibrium Thermodynamics* (North-Holland, Amsterdam, 1969).
- [23] L. D. Landau and E. M. Lifschitz, Fluid mechanics, *Course of Theoretical Physics*, 2nd English ed. (Pergamon Press, 1987) Vol. 6.
- [24] W. Weiss and I. Müller, Light scattering and extended thermodynamics, *Continuum Mech. Thermodyn.* **7**, 123 (1995).
- [25] C. Cattaneo, Sur une forme de l'équation de la chaleur éliminant la paradoxe d'une propagation instantanée, *Compt. Rendu* **247**, 431 (1958).
- [26] M. Y. Alievskii and V. Zhdanov, Transport and relaxation phenomena in polyatomic gas mixtures, *Zh. Eksp. Teor. Fiz.* **55**, 221 (1968) [*Sov. Phys. JETP* **28**, 116 (1969)].
- [27] H. Grad, On the kinetic theory of rarefied gases, *Commun. Pure Appl. Math.* **2**, 331 (1949).
- [28] M. Born and E. Wolf, *Principles of Optics: Electromagnetic Theory of Propagation, Interference and Diffraction of Light* (Elsevier, Amsterdam, 2013).
- [29] D. R. Lide, *CRC Handbook of Chemistry and Physics* (CRC Press, Boca Raton, 2004), Vol. 85.
- [30] N. Bridge and A. Buckingham, Polarization of laser light scattered by gases, *J. Chem. Phys.* **40**, 2733 (1964).
- [31] K. T. Chung, Dynamic polarizability of helium, *Phys. Rev.* **166**, 1 (1968).
- [32] N.-J. Bridge and A. D. Buckingham, The polarization of laser light scattered by gases, in *Optical, Electric and Magnetic Properties of Molecules* (Elsevier, Amsterdam, 1997), pp. 105–120.
- [33] Y. Yokomizu, T. Kobayashi, and T. Matsumura, Particle composition and heat capacity of high-temperature SF₆ present at constant volume: Discussion on formula expressing relationship between constant-pressure and constant-volume heat capacities, *IEEJ Trans. Electr. Electron. Eng.* **10**, 683 (2015).
- [34] W. F. Koehler, The ratio of the specific heats of gases, c_p/c_v , by a method of self-sustained oscillations, *J. Chem. Phys.* **18**, 465 (1950).
- [35] S. Chapman, T. G. Cowling, and D. Burnett, *The Mathematical Theory of Non-uniform Gases: An Account of the Kinetic Theory of Viscosity, Thermal Conduction and Diffusion in Gases* (Cambridge University Press, Cambridge, 1990).
- [36] J. Bzowski, J. Kestin, E. A. Mason, and F. J. Uribe, Equilibrium and transport properties of gas mixtures at low density: Eleven polyatomic gases and five noble gases, *J. Phys. Chem. Ref. Data* **19**, 1179 (1990).
- [37] C. L. Kong, Combining rules for intermolecular potential parameters. II. Rules for the Lennard-Jones (12–6) potential and the Morse potential, *J. Chem. Phys.* **59**, 2464 (1973).
- [38] S. U. Kim and C. W. Monroe, High-accuracy calculations of sixteen collision integrals for Lennard-Jones (12–6) gases and their interpolation to parameterize neon, argon, and krypton, *J. Comput. Phys.* **273**, 358 (2014).
- [39] E. A. Johnson, Light-scattering predictions in the two-temperature regime for disparate-mass gas mixtures, *Phys. Rev. A* **27**, 1146 (1983).
- [40] Z. Gu, M. O. Vieitez, E. J. van Duijn, and W. Ubachs, A Rayleigh-Brillouin scattering spectrometer for ultraviolet wavelengths, *Rev. Sci. Instrum.* **83**, 053112 (2012).
- [41] Y. Wang, Ph.D thesis, Spontaneous Rayleigh-Brillouin scattering in molecular gases, Vrije Universiteit Amsterdam, 2019.
- [42] M. Sneep and W. Ubachs, Direct measurement of the Rayleigh scattering cross section in various gases, *J. Quant. Spectrosc. Radiat. Transfer* **92**, 293 (2005).
- [43] Y. Wang, Y. Yu, K. Liang, W. Marques, W. van de Water, and W. Ubachs, Rayleigh-Brillouin scattering in SF₆ in the kinetic regime, *Chem. Phys. Lett.* **669**, 137 (2017).
- [44] M. G. Rodbard and G. M. Kremer, Kinetic theory for mixtures of polyatomic gases of rough spherical molecules, *Phys. Fluids A* **2**, 1269 (1990).